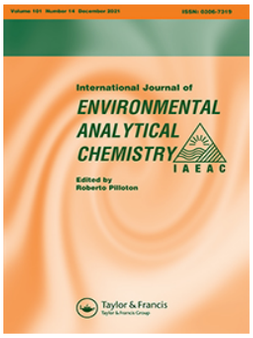

International Journal of Environmental Analytical Chemistry

ISSN: (Print) (Online) Journal homepage: https://www.tandfonline.com/loi/geac20

Use of new polymeric composites for preconcentration of trace Ag^{+} ions from the selected mushroom/vegetables by ultrasound-assisted cloud-point extraction coupled to microvolume UV-Vis spectrophotometry

H. B. Zengin

To cite this article: H. B. Zengin (2021) Use of new polymeric composites for preconcentration of trace Ag^{+} ions from the selected mushroom/vegetables by ultrasound-assisted cloud-point extraction coupled to microvolume UV-Vis spectrophotometry, International Journal of Environmental Analytical Chemistry, 101:14, 1978-2002, DOI: 10.1080/03067319.2019.1691186

To link to this article: https://doi.org/10.1080/03067319.2019.1691186

INTERNATIONAL JOURNAL OF ENVIRONMENTAL ANALYTICAL CHEMISTRY
2021, VOL. 101, NO. 14, 1978–2002
https://doi.org/10.1080/03067319.2019.1691186

Taylor & Francis
Taylor & Francis Group

ARTICLE

Use of new polymeric composites for preconcentration of trace Ag^+ ions from the selected mushroom/vegetables by ultrasound-assisted cloud-point extraction coupled to microvolume UV-Vis spectrophotometry

H. B. Zengin

Faculty of Sciences, Department of Chemistry, University of Cumhuriyet, Sivas, Turkey

ABSTRACT

The magnetic nano-composites based on the tris(hydroxymethl-methyl)aminomethane-modified maleic anhydride-co-styrene copolymers and Fe_3O_4 nano-particles were prepared as new potential chelating agents for ultrasound-assisted-cloud point extraction (UA-CPE) and pre-concentration of trace levels of Ag^+ ions from aqueous solutions. The structures of the nano-composites were characterised via FT-IR, ^{1}H-NMR and XRD analysis. After structural characterisation of composites, Ag^+ ions were detected by micro-volume UV-vis spectrophotometry at 347 nm. The variables affecting complex formation and extraction efficiency for separation/pre-concentration of the Ag^+ ions from various food matrices were evaluated and optimised in detail. Under the optimised conditions, the method shows a good sensitivity with linearity range from 10 to 350 µg L^{-1} and 4 to 160 µg L^{-1} for amidic and imidic composites, respectively, with a better correlation coefficient than 0.9825. The limits of detection, intra- and inter-day precision (as RSDs%) and recovery rates for six replicate determinations of Ag^+ ions at levels of 25 and 100 µg L^{-1} were 4.28/1.21 µg L^{-1}, 2.4–4.1% and 92–98% for the modified copolymers, respectively. The pre-concentration factor for Ag^+ ion from pre-concentration of 35-mL sample was 70. A significant matrix effect was not observed for the triplicate measurements of 100 µg L^{-1} Ag^+ in the presence of various interfering species below their maximum concentrations allowed in this method, for Ag^+ ions. The accuracy of the method was confirmed by analysis of the two certified samples. The method was successfully applied to determine low levels of Ag^+ ions in mushroom and vegetable samples, and satisfactory recoveries were obtained in the range of 91-97% with lower RSD than 5.1% for the spiked samples.

ARTICLE HISTORY
Received 26 September 2019
Accepted 27 October 2019

KEYWORDS
Ultrasound-assisted-cloud point extraction; tris modification; copolymers; micro-volume UV-vis spectrophotometry; Ag^+ ions; vegetables/mushrooms

1. Introduction

Silver ion is a very toxic substance as a metabolic inhibitor of lower life forms. Biochemically, the silver ion acts as an enzyme inhibitor [1]. According to one study, 'ionic silver is unique in comparison with other antibiotics in that it has no toxicity and carcinogenic activity' [2]. Silver ion is a disinfectant for non-spore-forming bacteria, such as *Salmonella* spp., *Staphylococcus* and *Escherichia coli*, at concentrations about 1,000

CONTACT H. B. Zengin hbzengin@gmail.com

times lower than the levels at which it is toxic to mammalian life [2]. This extreme mammalian-to-bacterial toxicity difference is the definition of an oligo-dynamic material. Silver does not occur regularly in animals or humans; but is present in air, water, soil and food. The average concentration of silver in water is 0.5 μg L^{-1}, while its concentration in soil is approximately 10 μg L^{-1} [3]. EPA lists silver as a Group D carcinogen (i.e. not carcinogenic in humans) and established an oral reference dose at a daily intake limit of 5 μg kg^{-1}. According to EPA, 'minimal dietary exposure may result from the use of silver in human drinking water systems' [4,5]. Therefore, due to its toxicity even at trace and ultra-trace levels, development of a highly sensitive and selective method is of great importance for the accurate and precise determination of silver in various sample matrices.

Some atomic spectrometric and chromatographic techniques such as inductively coupled plasma mass spectrometry (ICP-MS) [6,7], inductively coupled plasma optical emission spectrometry (ICP-OES) [8–10], graphite furnace atomic absorption spectrometry (GFAAS) [11,12], electrothermal atomic absorption spectrometry (ETAAS) [13,14], thermospray flame furnace atomic absorption spectrometry (TS-FFAAS) [15], flow injection flame atomic absorption spectrometry (FI-FAAS) [16], flame atomic absorption spectrometry (FAAS) [17–28], reverse-phase-high-performance liquid chromatography-photodiode array detection (RP-HPLC-PAD) [29], including spectrophotometry [30,31] have been developed for the determination of silver in different sample matrices. In order to lower the detection limit and to compensate for the matrix effect, a variety of pre-concentration processes have also been utilised prior to the analysis in combination with these detection tools. Those sample preparation techniques include solvent extraction or liquid-liquid extraction (LLE) [32], solid-phase extraction (SPE) [11,29], cloud point extraction (CPE) [7,14,17,18,20], precipitation [33], co-precipitation [34], floatation [35] and ultrasound-assisted extraction (UAE) [36] as well as further pre-concentration tools such as DLLM, IL-SDME, UASEME, SPE and CPE at different operation modes. However, most of these procedures are tedious, time consuming, require large volumes of toxic organic solvents and may also cause sample contamination in sample preparation step before analysis.

Among these techniques, the CPE procedure is a new and eco-friendly LLE technology and has especially gained large attention in separation science. The CPE is based on the clouding phenomena of surfactants [37]. The changes in the experimental operational parameters (e.g. solution pH, temperature, concentration and time) lead to phase separation. It can be used to separate the hydrophobic and hydrophilic materials from matrix, and it is economic, safe, environmental benign, efficient and convenient [38–41]. When this technique, which is also called as UA-CPE (or USA-EME), is assisted by ultrasound energy for the acceleration of various steps in analytical procedures such as homogenising and emulsion forming, the acceleration of the mass-transfer process between two immiscible phases is greatly facilitated. As a result, this leads to an increase in the extraction efficiency of the process within a minimum span of time [23,25,26,28]. In fact, this new approach offers many advantages such as simplicity, rapidity, a high enrichment factor, and safety and low cost due to consumption of very small amounts of toxic organic solvents.

Recently, the UA-CPE has been successfully used in separation, preconcentration and determination of Ag^{+} ions from water, dried-nuts and vegetable samples [25,26]. Especially, in SPE, to overcome drawbacks such as clogging of cartridges, being time–consuming, necessity of pump usage, low extraction efficiency resulted from particles aggregation and impossibility treatment of large sample volumes, magnetic solid-phase extraction (mSPE) has

been latterly appeared, and begun to be used preferably as a new SPE approach by researchers, using popular magnetic sorbents selectively to adsorb analyte(s) by chelation, ion-exchange and adsorption. These sorbents can be easily separated using an external magnetic force from an aqueous solution. Then, a suitable solvent or acidic solvent is used for desorption of analytes for further determination, depending on detection instrument. The magnetic nanoparticles (mNPs) are a kind of nanoparticles (NPs, ranging from 1 to 100 nm), which present paramagnetism and also possess unique reactivity, and large specific surface area due to its nano-nature. The different NPs like Fe, Ni, Co, and their oxides are used as the core of the sorbents in mSPE that among them magnetite, Fe_3O_4 is often used NPs. The pure MNPs are seldom directly used in extraction methods because of lack of functional groups to interact with the analyte(s), aggregation tendency resulting in loss of their magnetism, quick biodegradation, and easily oxidation in air [42,43]. Thus, the mNPs are coated by silane groups for preventing aggregation and oxidation by air and/or to functionalise them with different chelating groups, which make the sorbents suitable to interact with the analyte(s). The mNPs are functionalised by chelators such as 3-(trimethoxysilyl)-1-propantiol/2-amino-5-mercapto-1,3,4-thiadiazole [44], dopamine or glutathione [6], 3-(trimethoxysilyl)-1-propantiol and modified with 2-amino-5-mercapto-1,3,4-thiadiazole [8], ethylene glycol bis-mercaptoacetate/3-(trimethoxysilyl)-1-propanethiol [9], styrene-maleic anhydride copolymer [45], 2-mercaptobenzothiazole/SDS [46], including ion-imprinted polymer nanoparticles [23] and multiwalled carbon nanotubes microcolumn [47] and without modification for extraction process of Ag^+ ions. To provide an improvement in selectivity and sensitivity of the extraction process by UA-CPE, fast, easy, efficient and versatile separation capability of mNPs was combined with two copolymers modified with tris (2-hydroxymethyl) amino methane as chelator for pre-concentration of trace Ag^+ ions at micellar interface.

In the present study, we applied UA-CPE for the separation and preconcentration of Ag^+ ions from food matrices using a mixed surfactant, Triton X-114 plus CTAB as extractant and the modified and magnetised copolymers with tris and Fe_3O_4, respectively, followed by its micro-volume UV-vis spectrophotometric determination at 347 nm. The modified and magnetised copolymers were characterised by means of instrumental techniques such as FTIR, ^{1}H-NMR and XRD. The parameters influencing the efficiency of UA-CPE such as effects of pH, buffer volume, the concentrations of the mixed surfactant (Triton X-114 and CTAB) and the modified copolymers, electrolyte amount, incubation temperature and time were evaluated and optimised in detail. The developed UA-CPE/spectrophotometric method has been successfully applied to the accurate and reliable determination of the concentration of Ag^+ ions in the selected food samples.

2. Experimental

2.1. Reagents, standard solutions and samples

Ultra-pure water (resistivity of 18.2 MΩ cm) obtained by a Labconco water purification system (Kansas City, USA) was used throughout this study. All glass wares, pipettes and plastic tubes were cleaned by soaking in 5.0% (v/v) HNO_3 solution during one day, later were rinsed five times with ultra-pure water before starting of experiment. The standard working solutions of Ag(I) at μg L^{-1} levels used for calibration were prepared daily by diluting a 1000 mg L^{-1} metal stock solutions purchased from Merck (Darmstadt, Germany) with 0.2 mol L^{-1} HNO_3 solution

immediately before use. The calibration solutions of Ag(I) at μg L^{-1} levels were obtained daily by stepwise dilution of stock solution with water. The modified- and magnetised-amide and imide copolymer derivatives with tris (2-amino-2-hydroxymethyl-propane-1,3-diol) and magnetite (Fe_3O_4), respectively (as selective and sensitive chelating agents for free Ag^+ ions), was prepared by dissolution of their suitable amounts in acetone. All the ionic and non-ionic surfactants, cetyltrimethylammonium bromide and sodium dodecyl sulphate (CTAB and SDS, 3.0×10^{-3} mol L^{-1}) and olyethylene glycol *tert*-octylphenyl ether (Triton X-114, 5.0% (v/v)) as extractant, obtained from Sigma, were prepared by dissolving appropriate amounts of surfactant in 100 mL volumetric flasks, and vortexing a homogeneous clear solution when necessary. The pH of the sample solutions was adjusted with universal Britton-Robinson buffer (BR buffer, containing equal-molar concentration of phosphoric, boric acid and citric acids) (each, 0.04 mol L^{-1}, pH 10.0) buffer solution.

Vegetables (spinach, lettuce, lentils, leeks, parsley, white and red cabbage) and mushroom samples (edible wild and cultured mushrooms, three and two, respectively) were collected from local markets (Sivas, Turkey) to evaluate the applicability of the method. For accuracy studies, two standard reference materials (SRMs) supplied from National Institute of Standards and Technology (Gaithersburg, MD, USA) were analysed: SRM 1573a Tomato leaves and SRM 1643d Trace elements in water.

2.2. Instrument and apparatus

The absorbance measurements were performed in 1-cm quartz cells using a UV Shimadzu 160A spectrophotometer. The equipment permits multiple expansions in both absorbance and wavelength, and an accuracy of (±0.001) in absorbance readings. The cells with micro-capacity, 0.35–0.70 mL were used in the absorbance measurements at 347 nm. FT-IR spectra were taken using a Bruker (Alpha 12283105 model, Billerica, MA, Germany) spectrometer (with direct sampling at ATR mode without KBr pellet). ^{1}H-NMR spectra (in DMSO, D6, 400 MHz, single pulse) were recorded on a JEOL JNM-ECZ400S/L1 spectrometer (JEOL Ltd., Akishima, Tokyo, Japan) operating at 298 K with tetramethylsilane (TMS) as an internal standard. Chemical shifts (δ) are quoted in ppm and coupling constants (J) are measured in Hertz (Hz). The XRD pattern was recorded by Rigaku Miniflex 600 x-ray diffractometer using Ni-filtered Cu Kα radiation. The pH measurements were performed using a digital pH metre (Selecta-2001 plus, Barcelano, Spain) supplied with a glass-calomel electrode. A centrifuge (Hettich universal 320 model, Darmstadt, Germany) was used to speed up the phase separation. A programmable ultrasonic bath (UCP-10 model, Seoul, Korea) was used for incubation with temperature ranging from 0 to 80°C and ultrasound frequency of 40 kHz at power of 300 watts. An ultrasound agitator was used for acceleration of the mass transfer in the extraction process.

2.3. Synthesis of maleic anhydride-alt-styrene copolymer, MA-ST and modification with tris

10 g of maleic acid and 10 mL of styrene (at ratio of 1:1) was thoroughly heated by stirring with 0.02 g of 2,2′-azobisisobutyronitrile (AIBN as radical initiator) in 50 mL of benzene. At 75–80°C, the MA-ST copolymer formed in bulk, separated by decantation and dried. Half of the resulting product (5.0 g) was taken and thoroughly dissolved in DMF with magnetic

stirring. About 10 mL of tris [Tris buffer, $(HOCH_2)_3CNH_2$, pK_a: 8.07] for modification was added to the solution. The brown solution was heated to a deep red colour. After stirring for 24 hours, it was precipitated by addition of ethyl alcohol.

Imidation, which is also known as thermally removal of 1 mol H_2O from molecular structure, for other half of the product (5.0 g) was carried out by heating in DMF at a constant temperature of 150°C for 2 hours, and the resulting product was precipitated with aqueous NaCl solution. The resulting MA-ST and tris-modified MTAA-ST and MTI-ST copolymers were dissolved in THF; but MTI-ST did not dissolve in acetone and THF. It only swollen in THF to a certain extent. The imide copolymer was first suspended in THF, swollen, and then dissolved by adding water.

2.4. Synthesis of Fe3O4 NPs, and magnetisation of the modified copolymers, MTAA-ST and MTI-ST with Fe3O4

10 mmol of $FeCl_3.6H_2O$ and 5 mmol of $FeCl_2.4H_2O$ (at ratio of 2:1) were stirred in 20 mL of deionised water and heated at 65°C until dissolved in an ultrasonic bath (40 kHz, 300 W). 80 mL of 1.5 mol L^{-1} NH_4OH solution (until pH is 10) was then added to the mixture followed by dispersion under ultrasonic irradiation. Heating was continued for precipitation at 65°C for 1 hour under N_2 atmosphere. The co-precipitate, which is formed by reaction of $2Fe^{3+} + Fe^{2+} + 8OH^- \rightarrow Fe_3O_{4(k)} + 4H_2O$, was then washed several times with water to pH 7.0. After sonication, the resulting product was placed in gooch crucible with vacuum outlet connected to nuche conical flask (with capacity of 50 mL) for suction, filtered and dried under vacuum at 60°C for 24 hours [48].

For the reaction of tris-modified copolymers with Fe_3O_4 NPs, two separate 0.5 g Fe_3O_4 NPs were initially taken, each incubated separately in an ultrasonic bath at 25°C in THF and 1.0 g of tris-modified polymers (MTAA-ST and MTI-ST) were added to each. Each mixture was individually activated in an ultrasonic bath at 65°C for 24 hours. The resulting magnetic products were precipitated with aqueous NaCl solution, and then dried under vacuum at 60°C [48].

For imidation of the MTAA-ST copolymer, the MTAA-ST copolymer dissolved in DMF was heated in an oil bath at 150°C for about 3 hours. Initially, the yellow-orange colour changed to red-black after thermal treatment. The resulting product was precipitated in ethanol, and filtered and dried in a vacuum oven. From samples of the modified copolymeric structures converted to film, FT-IR spectra were taken, and imidation was verified by means of imide ring peaks appearing at 1778 and 1721 cm^{-1}. The mechanism of the synthesis of tris-modified copolymers, in Scheme 1, can be schematically given as follows:

2.5. Collection, and preparation of samples to analysis

The determinations of Ag(I) by spectrophotometry were evaluated by analysis of samples such as vegetable samples (spinach, lettuce, lentils, leeks, parsley, white and red cabbage) and mushroom (edible wild and cultured mushrooms, three and two, respectively). All the samples were supplied from a local supermarket in Sivas, Turkey.

First, the vegetable and mushroom samples (5.0 g) were washed thoroughly with ultra-pure water, dried at 90°C, and ground to pass a 200-mesh sieve. Five grams of the homogenised samples was transferred to a 100-mL flask. For wet acid digestion, 5.0 mL of 3.0 mol L^{-1} of HNO_3 and 5.0 mL of 1.0 mol L^{-1} $HClO_4$ were added to the sample and were then completed to

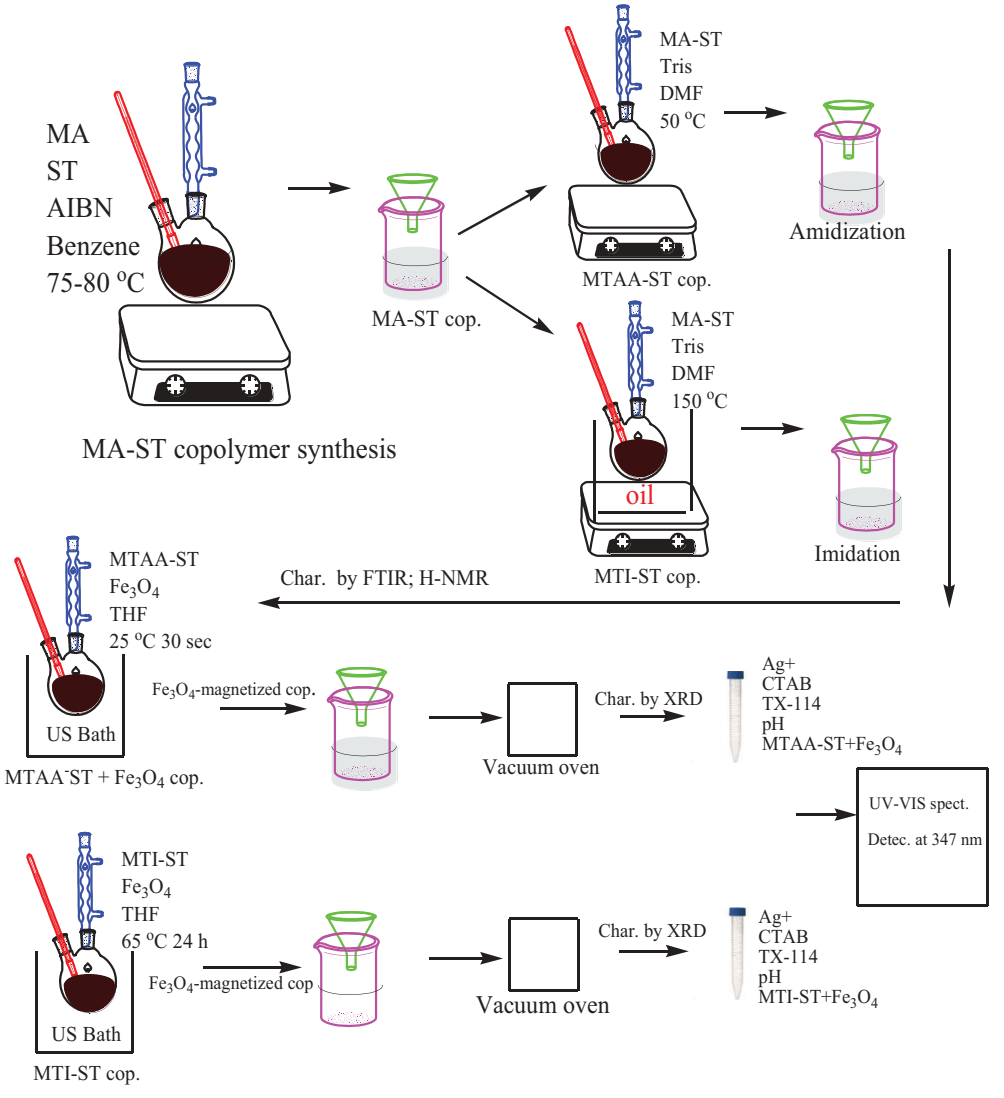

Scheme 1. The mechanism of the synthesis of tris-modified copolymers.
(i) By chelation
(ii) By ion-exchange as a function of pH

100 mL with the water. The mixtures were thoroughly sonicated and extracted under ultrasonic effect (300 W, 40 kHz) at 70°C for about 15 min. When necessary, same procedure has been repeated until a clear solution is obtained. After cooling to room temperature, the resulting mixtures were filtered using a membrane filter of 0.45-µm. The pH of the samples was adjusted to 7.0 using NaOH (0.5 mol L^{-1}) and completed to 50 mL with the water. Then, 10 mL of the pre-treated samples was submitted to UA-CPE procedure. The trace silver contents of the samples were determined via spectrophotometry using comparably both matrix-matched calibration curve and the standard addition method around the quantification limit to control the possible matrix effect. In a similar way, at least one blank solution

including suitable amounts of two SRMs was run for each sample in order to evaluate analyte contamination by reagents used. All the measurements and processing were performed at least in five times, and their mean values were considered.

2.6. UA-CPE procedure

A typical UA-CPE requires the following steps: an aliquot (3.0 mL) of the pre-treated sample solutions in two separate calibration ranges of 10–350 and 4–160 μg L^{-1} of Ag^{+} ions in optimisation step, and 35-mL of a sample solution containing no more than 0.5 μg of Ag(I) in pre-concentration step for two copolymers modified with tris, 0.25 mL of copolymers in acetone (up to 0.1 g/100 mL), 2.0 and 2.5 mL of 5% (v/v) of Triton X-114, 0.75 and 1.5 mL of 3×10^{-3} mol L^{-1} CTAB and 0.01 mol L^{-1} KNO_3, were sequentially mixed in a centrifuge tube of 50 mL, adjusted to pH 10 with 0.25, 1.0 mL of B-R buffer solution, and then completed to 50 mL by the water. The mixture was left to stand in an ultrasonic effect at 40°C for 5 min. After reaching to equilibria for efficient and complete complex formation, separation of the phases was achieved by centrifugation at 3000 rpm for 10 min. Due to become viscous of the surfactant-rich phase, the bulk aqueous phase was easily separated and decanted. To reduce the viscosity of the surfactant-rich phase for spectrophotometric measurements and facilitate the sample proceeding, it was diluted to a volume of 0.5 mL with acetone as diluent of both micellar phase and tris-modified copolymers. Finally, the Ag^{+} contents of the selected food samples were comparably evaluated by using both the matrix-matched calibration curve constructed by spectrophotometry at 347 nm against sample blank in extraction step and the standard addition method in order to control the possible matrix effect around detection limits when necessary.

2.7. Statistical analysis

For optimisation experiments, the standard deviations of the analytical signal were calculated for three replicate absorbance measurements at 347 nm, and represented as error bars. The intra-day and inter-day precision were expressed as the RSD for replicate measurements at two different concentration levels. The average and standard deviation of the analyte concentrations were calculated for analysis of each sample matrix. The obtained results for SRMs and samples were statistically evaluated by employing the Student's t test, and the calculated t-values were compared with the tabulated t-value for four and eight degrees of freedom at the 95% confidence level.

3. Results and discussion

3.1. Characterisation by FT-IR, ^{1}H-NMR and XRD of the copolymers modified and magnetised with tris and Fe_3O_4, respectively

By evaluation of FT-IR spectra in Figure 1(a), the two bands of 1854 and 1764 cm^{-1} are bands of the anhydride ring. The disappearance of the two bands at 1854 and 1764 cm^{-1} by the addition of tris to the MA-ST copolymer indicates that the anhydride ring was opened, and converted into the tris-maleamidic acid styrene copolymer derivative, MTAA-ST. The new peak at 1640 cm^{-1} corresponds to amide groups, whereas the peaks at

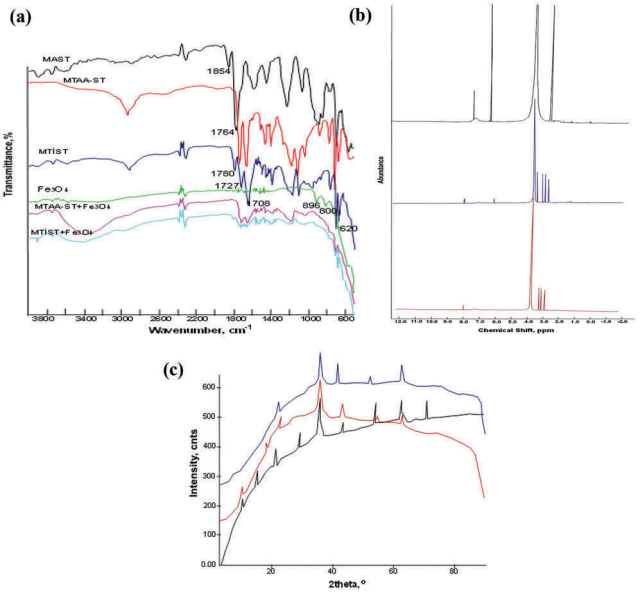

Figure 1. (a) ATR-FTIR spectra of copolymer and its derivatives before and after modification with tris and Fe_3O_4. (b)^{1}H-NMR spectra of: (a) Black: Only MA-ST (b) Blue: MTAA-ST and (c) Red: MTI-ST, showing their amidic and imidic derivatives of copolymer modified with tris. **(c)** X-ray powder diffraction patterns of: (a) Black: Only Fe_3O_4 (b) Red: MTAA-ST-Fe_3O_4 and (c) Blue: MTİ-ST-Fe_3O_4, showing bind of tris-modified amidic and imidic copolymers to Fe_3O_4 NPs.

1565 cm^{-1} and 1405 cm^{-1} correspond to carboxylate moieties. Surface wettability changed from hydrophobic to hydrophilic after tris modification which was associated with the opening of anhydride ring and addition of tris onto the polymeric structure. Subsequently, 1 mole of water was removed by thermally heating the tris-amidic acid styrene copolymers at 150°C for 5 hours to convert the structure to MTI-ST. This imidation process can be explained by the characteristic bands occurring at 1780, 1727 and 1708 cm^{-1}. The amidization and imidation processes can be also explained by shifting bands of MA-ST at 1217 and 1057 cm^{-1}, to characteristic group bands of 1384, 1250, 1163, 1097, 1023 cm^{-1} and 1387, 1170, 1009, 957 cm^{-1}, respectively, where the peaks centred at 1385 cm^{-1} and 1184 cm^{-1} are generally assigned to the (C–N) bond of the tertiary aromatic amine and the maleimide (C–N–C) stretch, respectively [48,49]. For the IR spectrum of Fe_3O_4, the absorption bands characteristically appeared at 580, 620, 800 and 896 cm^{-1} which can be attributed to absorption bands of Fe-O. In the IR spectra of the modified Fe_3O_4 nanoparticles, the characteristic absorption bands of the copolymers magnetised with Fe_3O_4 at 800 and 896 cm^{-1} were disappeared while the intensity of absorption band at 620 cm^{-1} gradually increased as a result of incorporation of Fe_3O_4 NPs into the copolymer matrix. This suggests the successful binding of tris-modified copolymers to Fe_3O_4 NPs [50].

In the ^{1}H-NMR spectra of copolymer (MA-ST) and the copolymer derivatives (MTAA-ST, MTI-ST) (δ, ppm) in Figure 1(b), broad overlapping peaks between 1.0 and 2.5 and peaks between 6.5 and 7.5 are due to methylene/methine and aromatic ring hydrogens of styrene, respectively. Methine protons of maleic anhydride appear between 3.5 and 4.0 as

the multiplet styrene/maleic anhydride ratio of the copolymer was calculated from the integration ratio of the peaks at 7.1–7.3 and 3.5–4.0. This ratio was about 0.95:1. As expected, an alternating copolymer was produced under the experimental conditions used in this work. The ^{1}H-NMR spectra of the copolymer derivatives (MTAA-ST, MTI-ST) showed characteristic peaks due to the hydroxyl groups bonded to tertiary tris-N atom (-OH), formed amidic – NH groups and carboxylic acid, -COOH groups as well as peaks of copolymer (MA-ST). Tris-modified copolymers showed a singlet peak and triplet peaks due to amidic -NH at 3.5 and hydroxyl – OH groups at 3.0 placing in environment of different functional groups (carboxylic acid, amide and phenyl groups) as well as typical peaks of the copolymer. However, peaks between 6.5 and 7.5 were partly shifted low and high magnetic areas, and their intensities clearly either decreased or completely disappeared by amidification and imidation process. The weak peaks appeared between 1.1 and 2.4 were due to methylene and methine protons of styrene units. The spectra were agreement with the proposed structure.

The powder XRD is a very powerful technique for characterising the structure of materials. To study the crystal structure of magnetic copolymers, the XRD patterns of the as-prepared-only Fe_3O_4 NPs and tris-modified copolymers, MTAA-ST and MTI-ST magnetised with Fe_3O_4 NPs are shown in Figure 1(c), respectively. As shown in Figure 1(c), there is only a broad diffraction peak in range of 20–30° (2θ), which is assigned to the reflection of tris-modified copolymers, indicating the amorphous nature of the copolymers. The XRD pattern of Fe_3O_4 NPs indicates their cubic spinel structures, and the presence of sharp and intense peaks confirms the formation of crystalline Fe_3O_4 NPs in Figure 1(c) [51]. The XRD pattern of the newly synthesised magnetic copolymers shows diffraction peaks at the Bragg angles of 25–30, 35, especially 35–40, 50, 55 and 65°, which are, respectively, ascribed to the known facets of the cubic spinel crystal planes of Fe_3O_4. After magnetisation of copolymers with Fe_3O_4, it is an evident that these peaks, especially a sharp peak in 35–40° as well as around 25, 55 and 65°, locally remained constant without changing, and Fe_3O_4 NPs incorporated into the tris-modified copolymer structures. So, the existence of Fe_3O_4 NPs in copolymer matrix is confirmed with a background noise, while the reflection peaks of the tris-modified copolymers in range of 20–30° are not disappeared. It may be due to the fact that after interacting with Fe_3O_4 NPs, they have been dispersed in structure of copolymers, in a manner that does not exhibit a regular structure, in terms of crystallinity. Shortly, this is an indicator of that the functionalisation process will not significantly affect the peak positions of the particles.

3.2. The mechanism for extraction and determination of trace Ag^+ ions

It is believed that the extraction process proceeds with two mechanisms, pH-dependent chelation and ion-exchange: The first one is predominantly based on the anionic chelate formation of Ag^+ ions with tris-modified copolymers at pH 10, and the subsequent ion-pair formation of anionic Ag-chelate with CTAB as counter ion in mixed micellar medium. The second one is based on formation of surface complexes by ion-exchange between Ag^+ ions and surface active sites of magnetite, Fe_3O_4 in which its zero-point charge pH_{pzc} is approximately 8.0 [52]. From prior studies conducted under the optimised reagent conditions, the absorbances of the resulting coloured ion-pair complex were measured at 347 nm, and correlated to the concentration of Ag^+ ions. The formation of extractable

hydrophobic neutral species, ion-pair complex and Ag-complex retained on the surface active sites of magnetite randomly dispersed in tris-modified copolymer phase by adsorptive forces, which is responsible for colour formation, in Scheme 2 where chelating ligands such as 2-mercaptobenzothiazole, ethylenediamine/3-amino-1,2,4-triazole-5-thiol, triethanolamine, 4-methylimidazole and sulphadiazine, including 2-hydrazinobenzothiazole for Hg^{2+} ions being a soft metal like Ag^{+} ions, for significant enhancement in the selectivity and sensitivity of the method is preferentially used in literature due to affinity to Ag^{+} ions [31,52–56] can be represented as follows:

Generally, the composite phase is an hydroxylated compound containing ionisable carboxyl, carbonyl and nucleophilic N-moiety, and its Ag-complexes are easily soluble in water due to be negatively charged, at hydrophilic character. Because of the solubility in water, the anionic Ag-complex cannot be quantitatively extracted into micellar phase. To improve the sensitivity, selectivity and linear working range of the method, the UA-CPE has been explored using cationic surfactant, CTAB as both a sensitivity enhancer and counter-ion. The UA-CPE

(i) By chelation

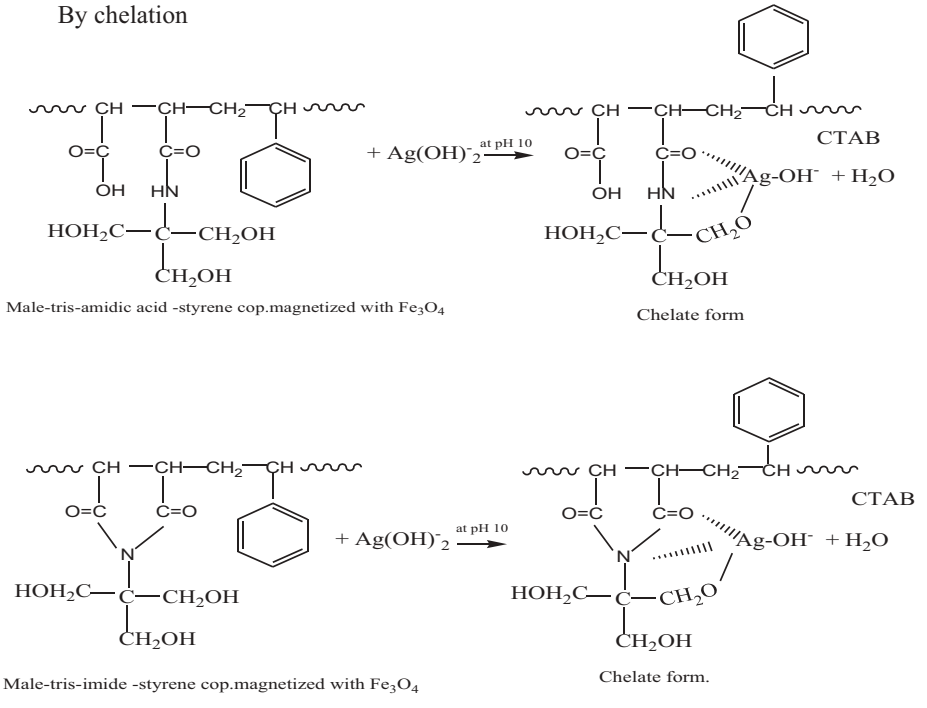

(ii) By ion-exchange as a function of pH

$$\text{Fe-OH} + \text{H}^+ \longrightarrow \text{Fe-OH}_2^+ \quad \text{If is lower than pH} < \text{pH}_{ZPC}$$

$$\text{Fe-OH} + \text{OH}^- \longrightarrow \text{Fe-O}^- + \text{H}_2\text{O} \quad \text{If pH is higher than pH}_{ZPC}$$

$$\text{Fe-OH} + \text{Ag}^+ \rightleftharpoons \text{Fe-O}^-\text{Ag}^+ + \text{H}^+ \quad \text{,at pH 10}$$

Scheme 2. The possible mechanism for extraction and determination of Ag^{+} ions.

can be used when the target species are hydrophobic in nature. Though the Ag-chelate complex is water soluble, it has been successfully extracted into surfactant-rich phase, and it can be explained through the following mechanism. When the concentration of surfactant is lower than the critical micelle concentration (CMC), only slightly soluble ion-pairs can form between anionic chelating ligand (herein, tris-base, pK_a: 7.08), chemically bound to copolymer at pH 10 and surfactant monomers causing turbidity [37]. Electrostatic interaction between the Ag-ligand complex and the mixed surfactant containing CTAB takes place through the negatively charged carboxyl and/or hydroxyl groups of the ligand and the positively charged head group of the surfactant molecule. The solubilising effect of the non-ionic surfactant begins at CMC and above, hence the neutral complexes get trapped into the core of micelles.

3.3. Optimisation of ternary complex formation and extraction process

To extent performance of the method to trace levels of silver, ternary complex of Ag^+ ions was extracted by UA-CPE method. The results show that by applying UA-CPE as a separation and pre-concentration tool, a good sensitivity could be obtained in spectrophotometric determination of Ag^+ ions. In this regard, to achieve maximum extraction efficiency, affecting parameters including pH, buffer volume, volume of the tris-modified- and Fe_3O_4-magnetised-amide and imide copolymers in acetone, volumes of triton X-114 and CTAB as extractant and auxiliary ligand, respectively, and salt effect on the extraction of the Ag-ternary complex in presence of CTAB as both sensitivity enhancer and ion-pairing surfactant were investigated and extensively optimised for triplicate measurements of 100 µg L^{-1} Ag^+ by using one-variable-at-a-time method.

3.3.1. Effect of pH and buffer concentration

It is of high importance to select appropriate chelating agent and metal ions to form a hydrophobic complex when metal ions are extracted by the CPE or UA-CPE. The complex is extracted to surfactant phase. The extraction efficiency depends on the acidity of the solution as the pH has an impact on the overall charges of the analyte, thus affecting the generation of the complex between the metal and the surface active functional groups. Therefore, the different pHs on the extraction efficiency of Ag^+ were investigated. UA-CPE of Ag^+ ions were carried out in the pH range of 3–11. The results are shown in Figure 2(a). The recovery for Ag^+ ions increased with increasing pH from 3 to 10, and reached a maximum with pH at 10. At low pHs, the low recoveries for Ag^+ ions were observed owing to the incomplete complex formation among reagents in reaction media. When the pH is in a range of 7–9, it could be a problem for the hydrolysis of Ag^+ ions due to minimal decrease or fluctuation in sensitivity [57]. At lower and higher pHs than 10, the low recoveries for Ag^+ ions were observed owing to the incomplete complex formation among reagents in reaction media and further formation of pH-dependent anionic hydroxo-complexes of Ag^+ ions like $Ag(OH)_2^-$, $Ag(OH)_3^{2-}$ and $Ag(OH)_4^{3-}$. Taking into account all these factors, a pH value of 10 as a result of participation of carbonyl, nucleophilic tris-N moiety, and pH-sensitive hydroxyl groups of on the chelating tris-modified copolymers in complex formation in the presence of CTAB in terms of extractable coordinately saturated-complex formation of Ag^+ ions at tetrahedral geometry was chosen for further studies.

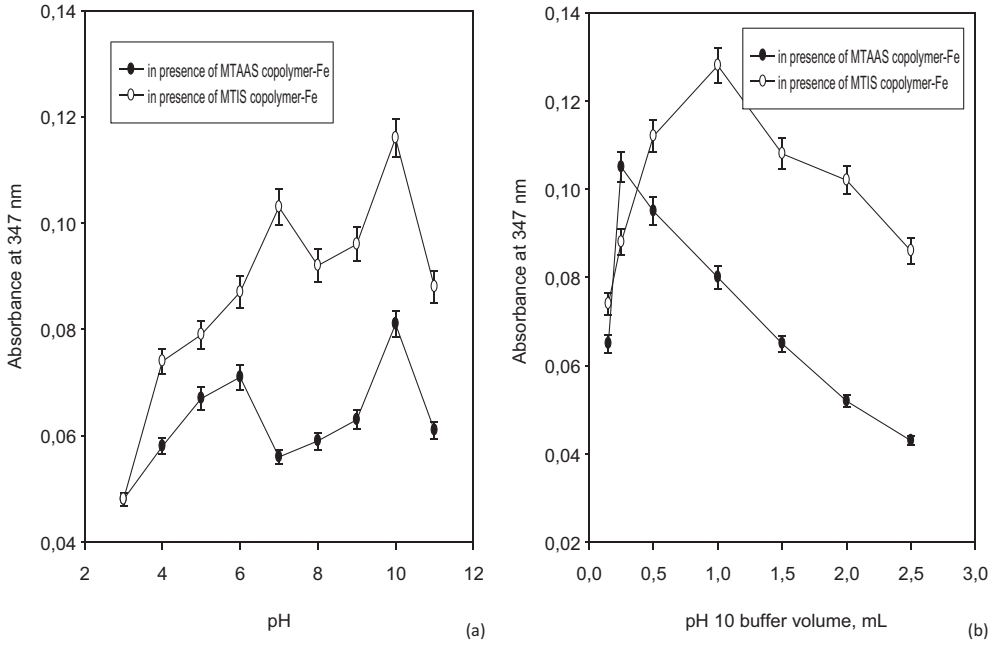

Figure 2. (a–b) Effect of (a) pH and (b) buffer volume of pH 10 on the sensitivity.

The effect of buffer concentration at pH 10 on the sensitivity in Figure 2(b) was also studied in volume range of 0.15–2.5 mL of B-R buffer solution at 0.04 mol L^{-1}. The best sensitivity was obtained at a volume of 0.25 and 1.0 mL for tris-modified amidic and imidic copolymers, respectively. At lower and higher buffer volumes, the sensitivity for Ag^{+} ions was gradually decreased. Therefore, a buffer volume of 0.25 and 1.0 mL for both copolymers was adopted as optimal.

3.3.2. Effect of tris-modified copolymer concentrations

Chelating agent is one of the important factors influencing the extraction efficiency. As can be seen in Figure 3, the extraction of Ag^{+} ions was carried out in the tris-modified copolymer concentration ranging from 0.025 to 0.5 mL. The extraction efficiency for Ag^{+} ions sharply increased with increase in chelating tris-modified copolymer concentration from 0.025 to 0.25 mL of their solutions at 0.1 g/100 mL in acetone, and reached a maximum sensitivity at a volume of 0.25 mL. However, when copolymer solution volume in acetone is higher than 0.25 mL, the extraction efficiency gradually decline. This decrease in signal could be due to extractable ion-pair formation of excess tris-modified chelating copolymers (in fact, containing pH- and concentration-dependent ionisable carboxyl and hydroxyl groups) with CTAB behaving such as an auxiliary ligand and/or counter ion in absence of Ag^{+} ions at pH 10, so as to lead to an increase in blank signal. Therefore, the optimum volume for tris-modified copolymers was considered as copolymer solution of 0.25 mL in acetone for further experiments.

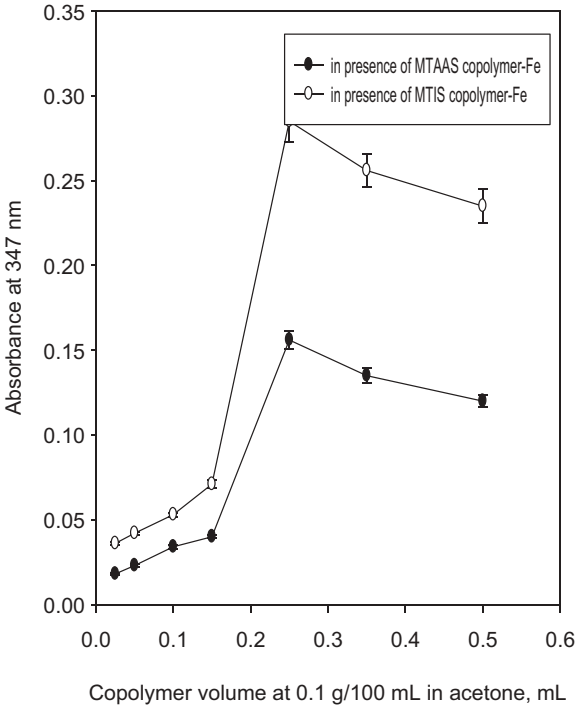

Figure 3. Effect of copolymer volume on the sensitivity.

3.3.3. Effect of CTAB and triton X-114 concentrations

The concentration of ionic and non-ionic surfactants used in the CPE or UA-CPE plays key roles. In presence of Triton X-114 as extractant in pre-concentration of trace Ag^{+} ions, at initial two ionic surfactants like CTAB and SDS in volume ranges of 0.1–5.0 mL at 3.0×10^{-3} mol L^{-1} were used as auxiliary ligand in extraction step. The sensitivity in Figure 4(a) linearly increased in ranges of 0.1–0.75 and 0.1–1.5 mL for tris-modified amidic and imidic copolymers, MTAAS and MTIS, reached to a maximum value at 0.75 and 1.5 mL and gradually decreased at higher volumes than 0.75 and 1.5 mL. This decrease in sensitivity may be due to increase in analyte blank as a result of extractable ion-pair formation between CTAB and tris-modified copolymers having pH-dependent ionisable carboxyl and hydroxyl groups. Therefore, CTAB volume of 0.75 and 1.5 mL was considered as optimal in this study. Due to its low sensitivity, SDS was not used in further studies.

Triton X-114 is one of the non-ionic surfactants extensively used in UA-CPE as extractant due to its advantages such as commercial availability with high purity, low toxicity and cost as well as high density of the surfactant-rich phase thus promoting the phase separation by centrifugation, relatively low cloud point temperature (CPT: 22–23°C) and low critical micelle concentration (CMC: 0.2 mmol L^{-1}). As a result, different concentrations of Triton X-114 in Figure 4(b) were investigated ranging from 0.25 to 3.0 mL at a concentration of 5.0% (v/v) for checking the extraction efficiency. The results are presented in Figure 4(b). The recovery for Ag^{+} ions increased with an increase in Triton X-114 concentration from 0.25 to 2.0 (or 2.5) mL for both tris-modified copolymers, and reached

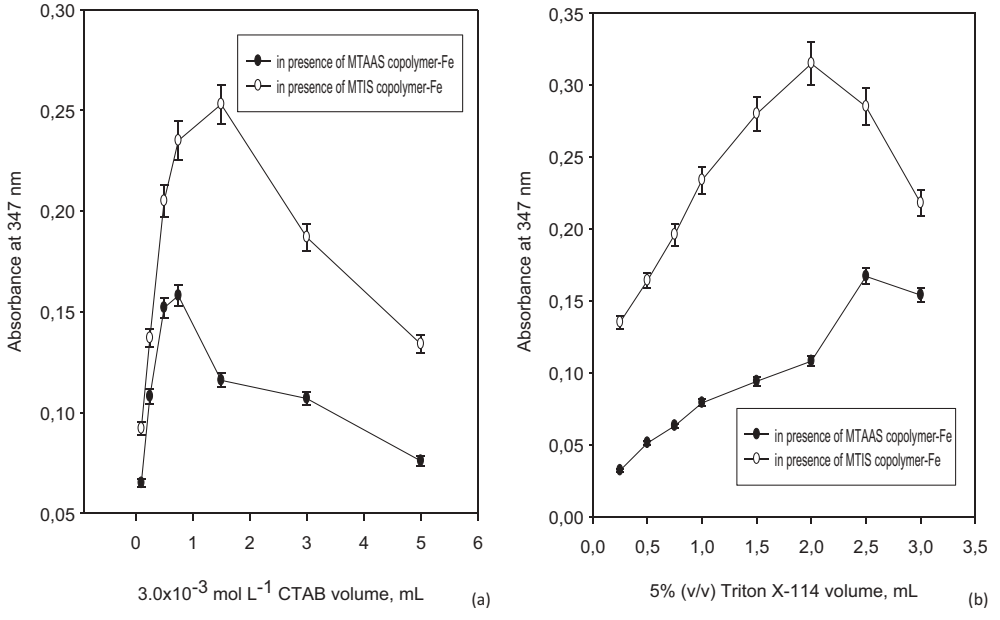

Figure 4. (a–b) Effect of (a) 3.0×10^{-3} mol L^{-1} CTAB and (b) 5.0% (v/v) Triton X-114 volumes on the sensitivity.

to a maximum at nearly a volume of 2.0–2.5 mL. The recovery gradually decreases when the concentration of Triton X-114 is higher than 2.0 or 2.5 mL. Such observations can be ascribed an increase in volume and viscosity of the micellar phase. Thus, a concentration of 2.0 and 2.5 mL at 5.0% (v/v) of Triton X-114 was used for subsequent experiments in order to achieve the greatest recoveries and thereby the highest extraction efficiency in spectrophotometric detection of Ag^{+} ions at 347 nm.

3.3.4. Effect of incubation time and temperature

The largest analyte pre-concentration factor is possible when the CPE process is performed with equilibration temperature well above the cloud point temperature of the micellar system. Therefore, the incubation temperatures ranging from 20°C to 55°C and time between 1 and 30 min in ultrasonic bath (300 W, 40 kHz) were studied. From the results, it has been observed that an equilibration time and temperature of 5 min and 40° C, respectively, is enough to reach the best sensitivity with maximum recovery for both tris-modified copolymers.

3.3.5. Effect of centrifugation time at 3000 rpm

Effect of centrifugation time on the UA-CPE procedure was investigated in range of 1–20 min for fast phase separation. From the results, it has been observed that the phase separation is completed in a centrifugation time of 10 min at 3000 rpm, and found to be enough for complete UA-CPE.

3.3.6. Effect of the ionic strength

In general, the addition of salt could decrease the solubility of aqueous sample phase and lead to enhancement of the partitioning of the analyte into the surfactant-rich phase by the 'salting out' phenomenon. The presence of salt can increase the incompatibility between the water structures in the hydration shells of analyte and surfactant macromolecules, which can reduce the concentration of 'free water' in the surfactant-rich phase and, consequently, reduce the volume of the phase [58]. In order to investigate the effect of ionic strength on the UA-CPE performance, various experiments were performed by adding different amounts of KNO_3 (0.005–0.05 mol L^{-1}). Other experimental conditions were kept constant during the analysis. The results showed that ionic strength has no significant effect on the pre-concentration factor up to a concentration of 0.01 mol L^{-1}. Thus, ionic strength was kept constant at a salt concentration of 0.01 mol L^{-1} in order to obtain reproducible and stable analytical signals.

3.3.7. Effect of diluents

In order to facilitate the detectability of the sample solution by spectrophotometry, it was necessary to decrease the viscosity of the surfactant-rich phase. Different solvents, such as acetone, acetonitrile, ethanol, methanol, and solutions of ethanol and methanol acidified with 0.2 mol L^{-1} HNO_3, were tried in order to select the one producing the best results regarding sensitivity, reproducibility, and stability of the signal. The best result was obtained with acetone. Aliquot of acetone (optimal 0.3 mL in the range of 0.1–1.5 mL) was added to the surfactant-rich phase after separation, in which the micellar phase is diluted to a volume of 0.5 mL for a pre-concentration factor of 70 from pre-concentration of optimal 35-mL sample (in the range of 5–50 mL). This amount of acetone was chosen to ensure a sufficient volume of the sample for maximum sensitivity. For smaller volumes, the reproducibility of the signals was very poor, whereas for higher volumes, there was a decrease in the signal due to dilution.

3.4. Analytical figures of merit

Under the optimal conditions, the analytical performance of the proposed method was studied in detail. This method allows the detection of Ag^+ ions by the solvent-based calibration curves (n: 6) in linear ranges of 4–160 and 10–350 μg·L^{-1} with correlation coefficients of 0.9825 and 0.9877, respectively, while it allows the detection of Ag^+ ions by the matrix-matched calibration curves (n: 6) in linear ranges of 4–160 and 10–300 μg·L^{-1} with correlation coefficients of 0.9855 and 0.9915, respectively. In order to minimise the possible matrix effect and instrumental signal fluctuations, matrix-matched standard calibrations curves, consisting of ten concentration levels (0, 5, 10, 25, 50, 100, 150, 200, 250, 300 and 350 μg L^{-1} for food extracts, were set up by spiking these different amounts of analyte into sample extracts. Blanks (samples with zero addition of the analyte) were simultaneously quantified using the standard addition, and the levels of analyte present in the samples were subtracted. To evaluate the performance of the calibration curves, all the samples were also analysed using a standard addition method based on spiked with two levels of analyte standards (0, 25, 100 μg L^{-1}) in both solvent and sample extracts. The spiked sample extracts and blanks were run consecutively in the instrument. It has been observed that there is not a significant difference between slopes of calibration curves

with a matrix effect of 6.7% and 18.7%, so as to cause enhancement in signal at 347 nm. The corresponding regression equations were found to be Abs: $(1.98 \pm 0.12)\times10^{-3}C + 0.0164 \pm 0.00080$ and Abs: $(5.25 \pm 0.28)\times10^{-4}C + 0.0172 \pm 0.00075$, respectively, while they were Abs: $(2.35 \pm 0.12)\times10^{-3}C + 0.0170 \pm 0.00090$ and Abs: $(5.60 \pm 0.30)\times10^{-4}C + 0.0180 \pm 0.00082$, respectively; where Abs is absorbance and C is the concentration of silver, respectively. The limits of detection and quantification (LODs and LOQs, 3σ/m and 10σ/m) were 1.21/4.04 and 4.28/14.3 $\mu g{\cdot}L^{-1}$ for the solvent-based calibration curves where σ is the standard deviation of twelve replicate measurements of the blank and m is the slope of the calibration curve while these values ranged from 1.15/3.83 to 4.39/14.6 $\mu g{\cdot}L^{-1}$ for the matrix-matched calibration curves. The intra-day and inter-day precision of (RSDs) of the extraction process for both calibration approaches was found to be in ranges of 3.1–5.1% and 3.8–6.5%, and 2.4–4.1% and 3.6–6.4% for Ag^{+} ions (25 and 100 $\mu g{\cdot}L^{-1}$, n = 5, 3 × 5) with a higher recovery than 91.5%. From pre-concentration of 35-mL sample solution, a pre-concentration factor of 70 was obtained. All the analytical parameters related to the pre-concentration system are extensively shown in Table 1.

3.5. Interference study

The effect of potential interference of some anionic and cationic species on the pre-concentration and determination of Ag^{+} ions was studied. In these experiments, aqueous solutions containing Ag^{+} (100 μg L^{-1}) with the addition of interfering ions were treated in tolerance ratios ranging from 1:25 to 1:2500, according to the recommended UA-CPE procedure under the optimised reagent conditions, and the results are given in Table 2. Table 2 depicts the tolerance limits of the diverse ions, *i.e.* interferent-to-analyte ratios in which the relative error was less than ±5.0% in terms of signal variation. Only an interference at low tolerance ratios (in range of 25–75) has been observed from CH_3Hg^{+}, Hg^{2+}, Cu^{+}, Cu^{2+}, Cd^{2+}, As^{3+} and Sb^{3+} ions forming a stable complex with the chelating tris-modifiedcopolymeric ligand. The interfering effect of CH_3Hg^{+}, Hg^{2+} and Cu^{+} ions up to150-250-folds excess over silver was greatly suppressed and improved using 1.5 mL of 0.02 mol L^{-1} pyridine solution as masking agent. The interference of As^{3+} and Sb^{3+} ions can be suppressed up to 350-fold after pre-oxidation of As^{3+} and Sb^{3+} to As^{5+} and Sb^{5+} with 0.01 mol L^{-1} H_2O_2 solution in alkaline medium. Also, the interference of Cu^{2+} and Cd^{2+} ions can be suppressed up to 500-fold using 0.2 mL of 0.05 mol L^{-1} $Na_2H_2P_2O_7$ solution or 0.25 mL of 0.01 mol L^{-1} $H_2C_2O_4$ solution. As can be seen from Table 2, it is clear that the developed UA-CPE method is relatively selective in terms of major species present in real samples. The recoveries in the range of 92.5–105.3% with a lower RSD than 4.1% were obtained for different metal to interfering ratios for the analyte studied. The results indicated that matrix did not affect the analyte absorbance signals at any of the studied interferent-metal tolerance ratios.

3.6. Accuracy of the method

The accuracy of the method was controlled by analysis of two certified samples, SRM 1573a Tomato leaves and SRM 1643d Trace elements in water with and without spiking at levels of 10 and 15 μg L^{-1} before extraction and spectrophotometric analysis. It can be seen that the results found by the present method in Table 3 are statistically in good agreement with their certified values where the experimental t-values are lower than the

Table 1. The analytical features of the micellar sensitive and selective spectrophotometric method based on extraction, pre-concentration and determination of trace amounts of Ag(I) with UA-CPE.

Fe_3O_4 magnetised-potential copolymeric chelating agents modified with Tris	Linear working range, µg L^{-1}	Regression coefficient, r^2	Regression equation	LOD, µg L^{-1}	LOQ, µg L^{-1}	Precision	Accuracy	
						Intra-day, RSD% (n: 5, for 25, 100 µg L^{-1})	Inter-day, RSD% (n:3 × 5, 25, 100 µg L^{-1})	Recovery %
By the solvent-based calibration curves (n: 6)								
By tris-modified amidic copolymer	10–350	0.9877	Abs: $(5.25 \pm 0.28)\times10^{-4}C + 0.0172 \pm 0.00075$	4.28	14.3	2.4–3.5	3.6–5.7	93.5–98.0
By tris-modified imidic copolymer	4–160	0.9825	Abs: $(1.98 \pm 0.12)\times10^{-3}C + 0.0164 \pm 0.00080$	1.21	4.04	2.8–4.1	3.5–6.4	92.0–97.0
By the matrix-matched calibration curves* (n: 6)								
By tris-modified amidic copolymer	10–300	0.9915	Abs: $(5.60 \pm 0.30)\times10^{-4}C + 0.0180 \pm 0.00082$	4.39	14.6	3.1–4.6	3.8–6.2	91.5–95.7
By tris-modified imidic copolymer	4–160	0.9855	Abs: $(2.35 \pm 0.12)\times10^{-3}C + 0.0170 \pm 0.00090$	1.15	3.83	3.5–5.1	3.8–6.5	92.0–95.5

*The linear calibration curves built between concentration and analytical signal as a function of increasing silver concentration under optimal conditions, so as to fall in the range of 5–350 µg L^{-1} before the extraction and pre-concentration of Ag^+ from sample matrix

Table 2. The possible matrix effect on the extraction of 100 μg L^{-1} Ag(I) by UA-CPE prior to analysis by spectrophotometry (n: 3).

Co-existing ions	Tolerance ratio, [Interferent]/[Ag^+]	Recovery %	RSD %
NH_4^+, K^+, Na^+, NO_3^-	2500	98.5–100.7	2.5
Ca^{2+}, Mg^{2+}, Sr^{2+}, NO_2^-, F^-	2000	98.5–100.6	2.5
Ba^{2+}, Cl^-, SO_4^{2-}, Acetate, Oxalate	1500	97.0–101.5	3.2
Al^{3+}, Fe^{3+}, Co^{2+}, Ni^{2+}	1000	98.0–101.3	2.0–3.5
Fe^{2+}, HCO_3^-, Br^-, Tartrate, 5-Sulfosalycilic acid	750	95.0–98.5	27–3.5
Zn^{2+}, EDTA, Ascorbic acid	500	92.5–95.5	3.4
Mn^{2+}, MoO_2^{2+}, VO^{2+}, VO_2^+, Cr^{3+}, Urea	350	93.0–97.5	3.0–4.1
Pb^{2+}, Bi^{3+}, I^-	250	96.5–98.2	2.8
As^{5+}, Sb^{5+}	200	95.0–96.5	3.5
$As^{3+,b}$, $Sb^{3+,b}$	75 (350)	92.5–94.0	2.3
$Cu^{2+,c}$, $Cd^{2+,c}$	50 (500)	95.0–97.2	2.8
$Hg^{2+,a}$, $Cu^{+,a}$	35 (250)	102.5–104.1	2.5
$CH_3Hg^{+,a}$	25 (150)	103.2–105.3	3.5

[a] By using 1.5 mL of 0.02 mol L^{-1} pyridine solution as masking agent
[b] After pre-oxidation of As^{3+} and Sb^{3+} to As^{5+} and Sb^{5+} with 0.01 mol L^{-1} H_2O_2 solution in alkaline medium
[c]By using 0.2 mL of 0.05 mol L^{-1} $Na_2H_2P_2O_7$ solution or 0.25 mL of 0.01 mol L^{-1} $H_2C_2O_4$ solution

Table 3. The analytical accuracy and/or validity of the developed method for trace amounts of Ag(I) in two CRMs (n: 5).

CRMs	Spiking level, μg L^{-1}	Certified value, μg kg^{-1} or μg L^{-1}	[a]Observed value, μg kg^{-1} or μg L^{-1}	RSD %	Recovery %	Student's t-test [b],t_{exp}
SRM 1573a Tomato leaves	-	17.0 ± 0.4	17.4 ± 0.6	3.4	-	1.49
	10		26.7 ± 0.9	3.4	93.0	
	15		31.8 ± 1.0	3.1	96.0	
SRM 1643d Trace elements in water	-	1.27 ± 0.06	1.25 ± 0.05	4.0	-	0.89
	10		10.9 ± 0.4	3.7	96.5	-
	15		15.8 ± 0.5	3.2	97.0	-

[a] The average plus its standard deviation of five replicate measurements using the proposed method
[b] The experimental t -values calculated by using $t = N^{1/2}(\mu - x_{average})/s$ for five replicate measurements at confidence interval of 95%in which the critical t-value is 2.31 for 4 degrees of freedom at confidence interval of 95%

critical t-value of 2.31 for 4 degrees of freedom at confidence interval of 95%. Also, after spiking, it is clear that recovery and precision levels can be quantitatively accepted with lower RSD than 4.0% and higher recovery rate than 93% for five replicate measurements.

3.7. Analytical applications of the method

The proposed method was applied for the determination of low levels of Ag^+ ions in food samples. The results are shown in Tables 4 and 5. It was found that silver at low ppb levels were observed in food samples studied. The accuracy of the method was verified in term

Table 4. The intra- and inter-day accuracy and precision studies of Ag(I) levels measured in the selected two quality control samples.

		Intra-day (n: 5)			Inter-day (n: 3 × 5)		
Sample	Added, μg kg^{-1}	Found, μg kg^{-1}	Recovery %	RSD %	Found, μg kg^{-1}	Recovery %	RSD %
Cultured mushroom	-	7.8 ± 0.3	-	3.8	8.4 ± 0.4	-	4.8
	10	17.3 ± 0.6	95	3.5	17.5 ± 0.7	91	4.0
Lettuce	-	4.5 ± 0.2	-	4.4	4.3 ± 0.2	-	4.7
	10	13.7 ± 0.5	92	3.6	13.6 ± 0.6	93	4.4

Table 5. The analysis results of trace levels of Ag(I) in the selected vegetable and mushroom samples by the developed spectrophotometric method (n: 5).

		By the matrix-matched calibration approach			By the standard addition method			
Sample	Added, μg kg^{-1}	[a]Found, μg kg^{-1}	Recovery %	RSD %	[a]Found, μg kg^{-1}	Recovery %	RSD %	Student's t-test[b], t_{exp}
Vegetable samples								
Spinach	-	1.40 ± 0.06	-	4.3	1.45 ± 0.06	-	4.1	1.32
	10	10.8 ± 0.4	94	3.7	11.1 ± 0.4	96.5	3.6	-
Lettuce	-	4.4 ± 0.2	-	4.5	4.6 ± 0.2	-	4.3	1.58
	10	14.0 ± 0.5	96	3.6	14.3 ± 0.5	97	3.5	-
Lentils	-	2.90 ± 0.12	-	4.1	3.00 ± 0.12	-	3.8	1.32
	10	12.5 ± 0.5	96	4.0	12.7 ± 0.5	97	3.9	-
Leeks	-	5.1 ± 0.2	-	3.9	5.3 ± 0.2	-	3.7	1.58
	10	14.6 ± 0.5	95	3.4	14.8 ± 0.5	95	3.4	-
White cabbage	-	7.5 ± 0.3	-	4.0	7.7 ± 0.3	-	3.9	1.05
	10	17.0 ± 0.6	95	3.5	17.2 ± 0.6	95	3.5	-
Red cabbage	-	8.5 ± 0.4	-	4.7	8.7 ± 0.4	-	4.6	0.79
	10	17.8 ± 0.7	93	3.9	18.1 ± 0.6	94	3.3	-
Parsley	-	9.3 ± 0.4	-	4.3	9.1 ± 0.4	-	4.4	0.79
	10	18.5 ± 0.7	92	3.8	18.3 ± 0.7	92	3.8	-
Edible wild and cultured mushroom samples								
Wild $mushroom_1$	-	15.7 ± 0.7	-	4.4	16.0 ± 0.7	-	4.4	0.68
	10	25.1 ± 1.0	94	4.0	25.6 ± 1.0	96	3.9	-
Wild $mushroom_2$	-	12.1 ± 0.6	-	5.0	11.8 ± 0.6	-	5.1	0.79
	10	21.5 ± 0.8	94	3.7	21.4 ± 0.8	96	3.7	-
Wild $mushroom_3$	-	18.2 ± 0.8	-	4.4	18.5 ± 0.8	-	4.3	0.59
	10	27.5 ± 1.0	93	3.6	27.8 ± 1.0	93	3.6	-
Cultured $mushroom_1$	-	8.5 ± 0.4	-	4.7	8.7 ± 0.4	-	4.6	0.79
	10	17.5 ± 0.7	90	4.0	17.8 ± 0.7	91	3.9	-
Cultured $mushroom_2$	-	7.2 ± 0.3	-	4.2	7.5 ± 0.3	-	4.0	1.58
	10	16.7 ± 0.6	95	4.1	16.8 ± 0.6	93	3.6	-

[a]The average plus its standard deviation of five replicate measurements obtained by using two calibration approaches
[b]The experimental t-values were calculated by using $t = (x_{average,1} - x_{average,2})/s_{pooled} \times [(N_1 + N_2)/(N_1 \times N_2)]^{1/2}$ for five replicate measurements at confidence interval of 95%in which the critical t-value is 2.78 for 8 degrees of freedom at confidence interval of 95%

of statistical evaluation by means of Student's t-test of experimental data based on matrix-matched calibration curve and standard addition method, and recovery rates obtained from replicate measurements with and without spiking. The selected food samples were spiked with the target analyte at concentration levels of 10 μg L^{-1} including two quality control samples, before extraction and analysis. Extractions were carried out under the optimum extraction conditions, intra-day and inter-day accuracy and precision measurement results (as the percent recoveries and RSDs, n: 5, 3 × 5) are summarised in Tables 4 and 5. Accuracy (percentage recovery values) from matrix-matched calibration approach and standard addition method were in the range of 90–97% with their respective RSDs lower than 5.1%. From direct measurement results without spiking via two calibration approaches to compensate for the matrix effect in spectrophotometric analysis, it has been observed that the Ag(I) contents of the vegetable samples are in range of 1.40–9.30 and 1.45–9.1 μg kg^{-1}, respectively, while the Ag^+ contents of mushroom samples are in range of 7.2–18.2 and 7.5–18.5 μg kg^{-1}, respectively. There is not statistically a significant difference between the measurement results obtained by two calibration approaches from comparison of two average value. The results clearly show that the proposed UA-CPE method can be successfully applied for the recovery, pre-concentration

and determination of Ag(I) in the selected food samples, which further indicates the capability of the method in the determination of the trace amounts of Ag^+ in real samples containing different matrices under the optimal conditions.

3.8. Comparison of the method with other reported methods

The method was compared with a variety of detection methods that had recently been reported in the literature for extraction, pre-concentration, and determination of silver from sample matrices. The analytical performance properties of the method are given in Table 6. As can be seen from Table 6, it is evident that the method has quantitatively the reasonable linear working ranges for the modified- and magnetised-amidic and imidic copolymers with tris and Fe_3O_4. Moreover, the detection limits of the method, 1.15/4.39 and 1.21/4.28 μg L^{-1} for the two calibration approaches, is either better than or comparable with that of other methods which even use more sensitive detection techniques such as ICP-OES, ICP-MS and FAAS after pre-concentration with CPE, UA-CPE, USA-EME, DLLM, IL-SDME, and SiAP-based SPE [7,10,18,20–22,24,25,27,28]. In fact, the sensitive detection techniques such as ICP-MS, ICP-OES, ETAAS and/or GFAAS, including RP-HPLC-PAD, require expert user in his/her research area, including expensive, complicated, and time-consuming sample cleaning, extraction, and separation procedures at suitable elution mode. Shortly, the method, based on sensitive and selective detection of low levels of Ag^+ ions by spectrophotometry at 347 nm, can be evaluated as simple, cost-effective, eco-friendly, accurate, and reliable analytical detection tool with a pre-concentration factor of 70-fold from pre-concentration of 35-mL sample because it uses low-volume non-toxic organic solvents and shows more favourable properties as simplicity, quickness, and relatively low cost when compared to dual CPE, SPE, and different modes of SPE like magnetic SPE and UA-dispersive SPE using magnetic particles and ion imprinted polymers, requiring generally longer analysis time, high aqueous sample volume, and manipulation of sample as well as possibility of contamination, loss of analyte, risk of degradation of compounds during long analysis time, and less accuracy and precision. In addition, the method gave comparably accurate and reliable results in terms of linearity, accuracy, and intra-day and inter-day precision and provided an evidence of spectrophotometry's feasibility as an alternative approach to routine quality control of levels of low amounts of silver in other sample matrices.

4. Conclusions

In the current work, new synthesised and characterised amidic and imidic copolymers modified and magnetised with tris and Fe_3O_4, respectively, which are used as potential chelating ligands for sensitive and selective complexation of Ag^+ ions in the presence of matrix components at pH 10 prior to its extraction, pre-concentration, and determination by UA-CPE combined with spectrophotometry have resulted in a significant increase in the sensitivity, limit of detection, selectivity and enhancement in the popularity of micro-volume UV-Vis spectrophotometry besides the solvent-free extraction of toxic metals from complex matrices. The method provides the possibility of simple, cost-effective, accurate and reliable determination of Ag^+ with comparable results of those of direct HPLC and FAAS techniques, and it can be considered as an alternative economic tool to

Table 6. Comparison of analytical features of the proposed method and the other methods reported for determination of trace levels of Ag^+ ions in different sample matrices.

Sample matrix	Pre-concentration tool*	Detection technique*	Linear working range, μg L^{-1}	Detection limit, μg L^{-1}	PF (or EF)	Recovery %	RSD %	Extraction time, min	References
Tap water, lake and seawater	GMPs	ICP-MS	2–10	0.4	250	>97	<5	-	[6]
Antibacterial products, environmental Waters	CPE	ICP-MS	-	10 (LOQ for Ag^+)	-	71.7–103	1.7	35	[7]
Various waters	mSPE	ICP-OES	-	0.12	194	84.3–107	3.62–5.31	14	[8]
Rice, canned tuna fish, and tea leaves	mSPE	ICP-OES	-	0.07	240	96.2	2.8–4.1	15	[9]
Antibacterial products	SiAP-based SPE	ICP-OES	10–300 mg L^{-1}	4.6	-	>90	<3	15	[10]
Biological, water and soil samples	SPE	GFAAS	0.01–120	0.00085	300	89–104	<3.2	-	[11]
Environmental waters	LA-mSPE	GFAAS	20–800 ng L-1	7.5 ng L^{-1}	100	80.5–114	6.4	25	[12]
Environmental waters	Ligandless CPE	ETAAS	5–100 ng L-1	1.2 ng L^{-1}	60	97.5–101.7	4.2	10	[13]
Waters and lixiviates	CPE	ETAAS	0.005–10	0.002–0.15	242	95–104	≤4.6	15	[14]
Soil, marine sediment and ore samples	d-CPE	TS-FFAAS	0.7–20	0.2	21	95–118.5	5.5–15.6	15	[15]
Radiology film, hair, nails and waters	IIP-based SPE	FI-FAAS and LSPRP	0.4–25, 3–30	0.06, 0.5	320, 312	94.7–102, 94–106	2.9, 10.3	35	[16]
River water, tap water	CPE	FAAS	1-500	0.3	33	98.5–101.8	1.1–3.6	40	[17]
Complicated sample matrices	CPE	FAAS	-	1.4	30 (42)	96–103.2	2.1–3.6	55	[18]
Water	Single step/ multiple step-CPE	FAAS	10-150	0.52, 0.58	45, 42	97.2–99.5	≤2.5	60	[19]
Different waters and photographic washing	CPE	FAAS	10-200	2.2	46 (20)	>99	2.4–2.6	20	[20]
Waters, tea and pepperbush	DLLM	FAAS	50–800	30.4	73.2	95–96.5	3.2	6	[21]
Natural waters	IL-SDME	FAAS	10–500 ng L-1	4	71	96–105.4	4.2	12	[22]
Natural waters, photographic emulsion	UA-DSPE-IIP	FAAS	0.5–600	0.09	-	96.2–105.7	<3	<10	[23]
Water samples	Ligandless DLLM	FAAS	5–2000	1.2	16	98–106	1.5	5	[24]
Water samples	UA-CPE	FAAS	10–800	2.7	20	97.8–100.4	3.4	50	[25]
Dried nuts and vegetables	UA-CPE	FAAS	0.08–90	0.02	50 (103)	95–103	2.2–3.6	30	[26]

(*Continued*)

Table 6. (Continued).

Sample matrix	Pre-concentration tool*	Detection technique*	Linear working range, μg L^{-1}	Detection limit, μg L^{-1}	PF (or EF)	Recovery %	RSD %	Extraction time, min	References
High-purity salts and artificial seawater	One step displacement CPE	FAAS	5–450	1.0	50 (24)	95–106	2.6	15	[27]
Well water and photographic film	USA-EME	FAAS	0.055–1.5 mg L^{-1}	6.79	9.8	98.5	5.5	19	[28]
Waters	SPE	RP-HPLC-PAD	0.6–1000	0.004	-	92–106	1.9–3.2	10	[29]
Different sample matrices	CPE	Spectrophotometry	0.3–5	0.095	25 (325)	98.3–102	1.25 (for 3 μg L^{-1}, n:6)	10	[30]
Radiology film and environmental matrices	DLLM	Microvolume UV-vis spectrophotometry	0.5–105	0.2	54	93.2–101.1	1.7–3.5	10	[31]
Vegetables and mushroom	UA-CPE	Microvolume UV-vis spectrophotometry	10-350 (10–300), 4–160	1.15/4.39, 1.21/4.28	70 (48.5/36)	91.5–98.0	2.4–6.5	20	The present study

*PF (or EF): Sensitivity enhancement factor or pre-concentration factor; ICP-MS: Inductively coupled plasma mass spectrometry; ICP-OES: Inductively coupled plasma-optical emission spectrometry; ETAAS: Electrothermal atomic absorption spectrometry; GFAAS: Graphite furnace atomic absorption spectrometry; FI-FAAS: Flow injection-flame atomic absorption spectrometry; TS-FF-AAS: thermospray flame furnace atomic absorption spectrometry; FAAS: Flame atomic absorption spectrometry; RP-HPLC-PAD: Reverse-phase-high-performance liquid chromatography-photodiode array detection; LSPRP: localised surface plasmon resonance peak; USAEME: Ultrasound-assisted-emulsification microextraction; CPE: cloud point extraction; UA-CPE: Ultrasound-assisted-cloud point extraction; dCPE: Displacement cloud point extraction; mSPE: Magnetic solid-phase extraction; MD-μSPE: Magnetic dispersive-micro solid-phase extraction; MIIP-SPE: Magnetic ion imprinted nano-polymer-based solid-phase extraction; DLLM: Dispersive liquid-liquid microextraction; IL-DLLM: Ionic liquid-dispersive liquid-liquid microextraction; SDME: Single-drop microextraction.

the other sensitive, but expensive spectrometric and separation techniques such as ET-AAS and/or GFAAS, ICP-OES, ICP-MS and HPLC-PAD.

An UA-CPE procedure was developed for pre-concentration of Ag^{+} ions from sample matrix by using tris-modified amidic and imidic copolymers as a chelating agent, Triton X-114 and CTAB as extracting and sensitivity enhancer surfactants at pH 10, respectively. The developed protocol has been successfully employed for the determination of low levels of silver in vegetable and mushroom samples via microvolume UV-vis spectrophotometry at 347 nm. With respect to its achieved analytical parameters, the proposed method is simple, reasonably rapid, cost effective, low in LOD (1.15–4.28 $\mu g \cdot L^{-1}$), wide in linear ranges (4–160 and 10–350 $\mu g \cdot L^{-1}$) and highly reproducible (RSD <6.5%).

Acknowledgments

The financial support from the Scientific Research Projects of the Commission, CUBAP, University of Cumhuriyet (Sivas, Turkey), with code of F-604 is gratefully acknowledged. For the FT-IR, ^{1}H-NMR and XRD spectroscopic characterisation of the modified and magnetized copolymers with tris and Fe_3O_4, respectively, we would like to thank the technical staff of the Cumhuriyet University and the advanced technological research and application center (CUTAM) for the technical assistance and support. For allowing me to make use of all the facilities of the analytical research laboratory for conducting the present study, I would like to express my deepest gratitude to Prof. Dr. R. Gürkan. Also, thanks are due to him for his meaningful helps and valuable contributions in critical evaluation of the present article.

Compliance with ethics requirements

Author has no financial relationship with the organization that sponsored the research.

Disclosure statement

No potential conflict of interest was reported by the author.

Funding

This work was supported by the The Scientific Research Projects of the Commission, CUBAP, University of Cumhuriyet [Grant number F-604 project number].

ORCID

H. B. Zengin http://orcid.org/0000-0003-3861-6671

Ethical approval

This article does not contain any studies with human or animal subjects.

References

[1] J.L. Chambers, G.G. Christoph, M. Krieger, L. Kay and R.M. Stroud, Biochem. Biophys. Res. Comm. **59**, 70 (1974). doi:10.1016/S0006-291X(74)80175-0.
[2] K.I. Batarseh, J. Antimicrob. Chemother. **54**, 546 (2004).
[3] D.E. Newton, *Chemical Elements: From Carbon to Krypton*, 2nd ed. (Gale, Farmington Hills, MI, 2006).
[4] Agency for Toxic Substances and Disease Registry, Public Health Statement for Silver (December 1990) http://www.atsdr.cdc.gov/toxprofiles/phs146.html (accessed Feb 01 2005).
[5] A. Wadhera and M. Fung, Dermatol. Online J. **11**, 12 (2005).
[6] S.K. Mwilu, E. Siska, R.B.N. Baig, R.S. Varma, E. Heithmar and K.R. Rogers, Sci. Total Environ. **472**, 316 (2014). doi:10.1016/j.scitotenv.2013.10.077.
[7] J.-B. Chao, J.-F. Liu, S.-J. Yu, Y.-D. Feng, Z.-Q. Tan, R. Liu and Y.-G. Yin, Anal. Chem. **83**, 6875 (2011). doi:10.1021/ac201086a.
[8] M.H. Mashhadizadeh and Z. Karam, J. Hazard. Mater. **190**, 1023 (2011). doi:10.1016/j.jhazmat.2011.04.051.
[9] M. Mashhadizadeh, M. Amoli-Diva, M.R. Shapouri and H. Afruzi, Food Chem. **151**, 300 (2014). doi:10.1016/j.foodchem.2013.11.082.
[10] P. Anekthirakun and A. Imyim, Microchem. J. **145**, 470 (2019). doi:10.1016/j.microc.2018.11.008.
[11] G. Yang, W. Fen, C. Lei, W. Xiao and H. Sun, J. Hazard. Mater. **162**, 44 (2009). doi:10.1016/j.jhazmat.2008.05.007.
[12] B. Zhao, M. He, B. Chen and B. Hu, Talanta **183**, 268 (2018). doi:10.1016/j.talanta.2018.02.081.
[13] J.L. Manzoori, H. Abdolmohammad-Zadeh and M. Amjadi, J. Hazard. Mater. **144**, 458 (2007). doi:10.1016/j.jhazmat.2006.10.084.
[14] I. López-García, Y. Vicente-Martínez and M. Hernández-Córdoba, Spectrochim. Acta B **101**, 93 (2014).
[15] P. Wu, Y. Gao, G. Cheng, W. Yang, Y. Lv and X. Hou, J. Anal. At. Spectrom. **23**, 752 (2008). doi:10.1039/b719579f.
[16] S. Dadfarnia, A.M.H. Shabani, E. Kazemi, S. Ahmad, H. Khormizi, F. Tammadon and J. Braz, Chem. Soc. **26**, 1180 (2015).
[17] X. Yang, Z. Jia, X. Yang, G. Li and X. Liao, Saudi J. Biol. Sci. **24**, 589 (2017).
[18] M. Ghaedi, A. Shokrollahi, K. Niknam, E. Niknam, A. Najibi and M. Soylak, J. Hazard. Mater. **168**, 1022 (2009). doi:10.1016/j.jhazmat.2009.02.130.
[19] K.T.G. Naeemullah and M. Tuzen, J. Ind. Eng. Chem. **35**, 93 (2016). doi:10.1016/j.jiec.2015.12.022.
[20] F. Shemirani, R.R. Kozani and Y. Assadi, Microchim. Acta **157**, 81 (2007). doi:10.1007/s00604-006-0654-2.
[21] S. Bahar, Iranian J. Anal. Chem. **2**, 63 (2015).
[22] J. Abolhasani, M. Amjadi and E.G. Kalhor, J. Chem. Health Risks **3**, 29 (2013).
[23] M. Behbahani, F. Omidi and M.G. Kakavandi, Appl. Organometal. Chem. **31**, 1 (2017). doi:10.1002/aoc.3758.
[24] S.Z. Mohammadi, D. Afzali, M.A. Taher and Y.M. Baghelani, Talanta **80**, 875 (2009). doi:10.1016/j.talanta.2009.08.009.
[25] Z. Li, W. Zhen, Z. Tai, Y. Yang, J. Song and Y. Lian, Asian J. Chem. **25**, 2208 (2013).
[26] R. Gürkan, N. Altunay and E. Yıldırım, Food Anal. Methods **9**, 3218 (2016).
[27] Y. Gao, P. Wu, W. Li, Y. Xuan and X. Houa, Talanta **81**, 586 (2010). doi:10.1016/j.talanta.2009.12.038.
[28] G. Khayatian and B. Pourbahram, J. Anal. Sci. Technol. **7**, 1 (2016). doi:10.1186/s40543-016-0083-8.
[29] Q. Hu, G. Yang, Y. Zhao and J. Yin, Anal. Bioanal. Chem. **375**, 831 (2003). doi:10.1007/s00216-003-1828-y.
[30] M.A. Kassem, Anal. Methods **7**, 6747 (2015). doi:10.1039/C5AY01094B.
[31] B. Fouladvandi and S. Elhami, Iran. J. Chem. Chem. Eng. **36**, 163 (2017).

[32] T. Koh and T. Sugimoto, Anal. Chim. Acta **333**, 167 (1996). doi:10.1016/0003-2670(96)00221-8.
[33] O.D. Sant'Ana, A.L.R. Wagener, R.E. Santelli, R.J. Cassella, M. Gallego and M. Valcárcel, Talanta **56**, 673 (2002). doi:10.1016/S0039-9140(01)00604-X.
[34] X. Mao, H. Chen and J. Liu, Microchem. J. **59**, 383 (1998). doi:10.1006/mchj.1998.1581.
[35] M.S. Hosseini and H.M. Hamid, Bull. Korean Chem. Soc. **26**, 1529 (2005).
[36] I. De La Calle, N. Cabaleiro, M. Costas, F. Pena, S. Gil, I. Lavilla and C. Bendicho, Microchem. J. **97**, 93 (2011).
[37] M.D.A. Bezerra, M.A.Z. Arruda and S.L.C. Ferreira, Appl. Spectrosc. Rev. **40**, 269 (2005). doi:10.1080/05704920500230880.
[38] E.K. Paleologos, D.L. Giokas and M.I. Karayannis, Trac-Trends Anal. Chem. **24**, 426 (2005). doi:10.1016/j.trac.2005.01.013.
[39] P. Samaddar and K. Sen, J. Ind. Engin. Chem. **20**, 1209 (2014). doi:10.1016/j.jiec.2013.10.033.
[40] I. Hagarová and M. Urík, Curr. Anal. Chem. **12**, 87 (2016). doi:10.2174/1573411011666150601204931.
[41] M.F. Silva, E.S. Cerutti and L.D. Martinez, Microchim. Acta **155**, 349 (2006). doi:10.1007/s00604-006-0511-3.
[42] C.T. Yavuz, J.T. Mayo, W.W. Yu, A. Prakash, J.C. Falkner, S. Yean, L. Cong, H.J. Shipley, A. Kan, M. Tomson, D. Natelson and V.L. Colvin, Science **314**, 964 (2006). doi:10.1126/science.1131475.
[43] P.C. Lin, M.C. Tseng, A.K. Su, Y.J. Chen and C.C. Lin, Anal. Chem. **79**, 3401 (2007). doi:10.1021/ac070195u.
[44] M.H. Mashhadizadeh and Z. Karami, J. Hazard. Mater. **190**, 1023 (2011). doi:10.1016/j.jhazmat.2011.04.051.
[45] H. Abdolmohammad-Zadeh and M.A. Salmasi, Anal. Bioanal. Chem. Res. **5**, 23 (2018).
[46] M.A. Karimia, S.Z. Mohammadia, A. Mohadesia, A. Hatefi-Mehrjardi, M. Mazloum-Ardakanid, L. S. Korani and A.A. Kabir, Scientia Iranica **18**, 790 (2011). doi:10.1016/j.scient.2011.06.008.
[47] P. Biparva and M.R. Hadjmohammadi, Clean–Soil Air Water **39**, 1081 (2011). doi:10.1002/clen.v39.12.
[48] O.G. Atici, A. Akar and R. Rahimian, Turk. J. Chem. **25**, 259 (2001).
[49] W. Guo, L. Xiong, C.M. Reese, D.V. Amato, B.J. Thompson, P.K. Logan and D.L. Patton, Polym. Chem. **8**, 6778 (2017). doi:10.1039/C7PY01659J.
[50] S. Asgari, Z. Fakhari and S. Berijani, J. Nanostruct. **4**, 55 (2014).
[51] Z.E. Khalid, O.E.-S. Gamal and S.D. Ramy, Int. J. Min. Process **120**, 26 (2013). doi:10.1016/j.minpro.2013.02.007.
[52] E. Tombácz, A. Majzik, Z.S. Horivát and E. Illés, Rom. Rep. Phys. **58**, 281 (2006).
[53] L. Zhang, S. Yang, T. Han, L. Zhong, C. Ma, Y. Zhou and X. Han, Appl. Surf. Sci. **263**, 696 (2012). doi:10.1016/j.apsusc.2012.09.143.
[54] N. Altunay and R. Gurkan, Microchem. J. **147**, 999 (2019). doi:10.1016/j.microc.2019.04.022.
[55] E. Kazemi, S. Dadfarnia, A.M. Haji-Shabani, M.R. Fattahi and J. Khodaveisi, Spectrochim. Acta A Mol. Biomol. Spectrosc. **187**, 30 (2017). doi:10.1016/j.saa.2017.06.023.
[56] H.B. Zengin and R. Gürkan, Biol. Trace Elem. Res. **191**, 254 (2019). doi:10.1007/s12011-018-1614-5.
[57] R. Gürkan, N. Altunay and N. Gürkan, J. Iranian Chem. Soc **14**, 1033 (2017). doi:10.1007/s13738-017-1053-9.
[58] S.S. Arain, T.G. Kazi, J.B. Arain, H.I. Afridi, K.D. Brahman and Naeemullah, Microchem. J. **112**, 42 (2014). doi:10.1016/j.microc.2013.09.005.